Constraints on the frontal crustal structure of a continental collision from an integrated geophysical research: The central-western Betic Cordillera (SW Spain)

Ana Ruiz-Constan, A. Pedrera, J. Galindo-Zaldivar, J. Pous, J. Arzate, F. J. Roldan-Garcia, C. Marin-Lechado, F. Anahnah

Geochemistry Geophysics Geosystems G3

Article
Volume 13, Number 8
21 August 2012
Q08012, doi:10.1029/2012GC004153
ISSN: 1525-2027

Published by AGU and the Geochemical Society

Constraints on the frontal crustal structure of a continental collision from an integrated geophysical research: The central-western Betic Cordillera (SW Spain)

A. Ruiz-Constán
Géosciences Montpellier, Université Montpellier 2-CNRS, Place E. Bataillon, FR-34095 Montpellier, France (ruiz@gm.univ-montp2.fr)

A. Pedrera
Instituto Geológico y Minero de España, Ríos Rosas 23, ES-28003 Madrid, Spain (a.pedrera@igme.es)

J. Galindo-Zaldívar
Instituto Andaluz de Ciencias de la Tierra, CSIC–Universidad de Granada, ES-18071 Granada, Spain

Departamento de Geodinámica, Universidad de Granada, Campus Fuentenueva s/n, ES-18071 Granada, Spain (jgalindo@ugr.es)

J. Pous
Departament de Geodinàmica i Geofísica, Universitat de Barcelona, ES-08028 Barcelona, Spain (jpous@ub.edu)

J. Arzate
Centro de Geociencias, UNAM, Campus Juriquilla, 76220 Queretaro, Mexico (arzateja@gmail.com)

F. J. Roldán-García and C. Marin-Lechado
Instituto Geológico y Minero de España, Ríos Rosas 23, ES-28003 Madrid, Spain (fj.roldan@igme.es; c.marin@igme.es)

F. Anahnah
Departamento de Geodinámica, Universidad de Granada, Campus Fuentenueva s/n, ES-18071 Granada, Spain

[1] Mélange rocks outcrop widely in the central and western frontal sectors of the Betic Cordillera, as in many other collisional orogens where they form part of the accretionary wedges. Extrusion of Triassic plastic clays and evaporites was favored by the progressive accretion of the Betic External Zones, mixing rocks of different provenance and forming a synorogenic frontal mélange unit. MT data coupled with gravity data are a valid combined methodology to characterize the geometry of these mélange units, since the characterization of plastic rocks geometry is usually uncertain using seismic techniques. The results correlate well with known geological features (sedimentary basins, calcareous ranges, evaporitic rocks) and reveal the deep geometry. A resistive body, slightly dipping toward the SE, points to the continuity of the Iberian Massif below the Guadalquivir basin (2°) and the External Zones (6–8°). To the south, gravity models show the Iberian continental crust subducting below the Internal Zones with a roughly 20–35° slope. The main conductive bodies are related to the location of evaporitic rocks involved in the frontal mélange. They overlie the Iberian Massif and, southwards, the frontal Jurassic and Cretaceous limestone sequences of the External

and Median Subbetics. In this setting, thick plastic rock units placed above the foreland could act as a lubricant facilitating continental subduction, and being progressively accreted toward a frontal mélange.

Components: 9400 words, 10 figures.

Keywords: Gibraltar Arc; broadband magnetotelluric data; frontal mélange; gravity data.

Index Terms: 0925 Exploration Geophysics: Magnetic and electrical methods (5109); 1219 Geodesy and Gravity: Gravity anomalies and Earth structure (0920, 7205, 7240); 8038 Structural Geology: Regional crustal structure.

Received 19 March 2012; **Revised** 5 July 2012; **Accepted** 5 July 2012; **Published** 21 August 2012.

Ruiz-Constán, A., A. Pedrera, J. Galindo-Zaldívar, J. Pous, J. Arzate, F. J. Roldán-García, C. Marin-Lechado, and F. Anahnah (2012), Constraints on the frontal crustal structure of a continental collision from an integrated geophysical research: The central-western Betic Cordillera (SW Spain), *Geochem. Geophys. Geosyst.*, *13*, Q08012, doi:10.1029/2012GC004153.

1. Introduction

[2] In many collisional orogens, such as those forming the circum-Mediterranean belt, lithospheric flexure generated by the advance of the orogenic wedge toward the foreland has produced huge volumes of tectonic, sedimentary and/or diapiric mélanges [*Hsü*, 1968; *Moore and Karig*, 1980; *Raymond*, 1984; *Cowan*, 1985; *Pini*, 1999; *Vannucchi and Bettelli*, 2002]. These rocks, traditionally called 'chaotic', show high stratal disruption, including blocks of different ages and origin dispersed in an argillitic, sandy or ophiolitic matrix [*Camerlenghi and Pini*, 2009]. Although the surface description of these units is relatively simple, their genesis and sub-surface geometry are difficult to establish.

[3] Mélange units outcrop widely in the central and western frontal sectors of the Betic Cordillera, and were first defined as "Olistostromic units" by *Perconig* [1960–1962]. During their emplacement, the southern sediments of the Guadalquivir Foreland Basin were also deformed, and diverse hypotheses have been proposed to explain their provenance [*Fallot*, 1948; *García-Dueñas*, 1969; *Sanz de Galdeano*, 1975] and emplacement mechanism [*Flinch et al.*, 1996; *Berástegui et al.*, 1998; *Fernàndez et al.*, 1998]. These mélange units have a plastic behavior that highly controls the mechanism of accretion. Where plastic rocks, as clays or evaporates, are located at the detachment levels, the low angle of friction produces much thinner thrust wedges with a low foreland dip [*Lickorish et al.*, 1999]. The existence of carbonate rocks provides a buttress to the propagation of the thrust front generating a relatively thick orogenic wedge. In the study area, borehole data and seismic lines constrain the geometry of the northern part of this accretionary wedge, but its southern extension at depth is still poorly known. Moreover, determining the continuity and dip of the foreland below the detached frontal units is essential to elucidate the crustal structure.

[4] Since the 1970s, controlled-source seismic experiments have been performed with the aim of determining the geometry of the Guadalquivir foreland basin in detail, as well as the main features of the crustal structure and Moho depth below the Betic Cordillera and its foreland [*Banda and Ansorge*, 1980; *Medialdea et al.*, 1986]. More recently, magnetotelluric studies have been applied, but traditionally focusing on the crustal structure of the eastern Betics and the southwestern Iberian Massif [*Pous et al.*, 1999, 2004; *Martí et al.*, 2004, 2009; *Pedrera et al.*, 2009, 2010], or regional deep crustal and lithospheric structures [*Ruiz-Constán et al.*, 2010; *Rosell et al.*, 2011]. West of the 4°W meridian there is a lack of resistivity data focused on shallow crustal structures. New geophysical studies must be undertaken to better understand the behavior of this zone.

[5] In this study, we aim to achieve a more detailed image of the upper-middle crust of the central-western Betic Cordillera through analysis of new magnetotelluric and gravity data together with the compilation and reinterpretation of seismic reflection and borehole data. Their analysis provides the deep geometry of the Guadalquivir sedimentary foreland basin and the continuity at depth of the Iberian Massif foreland below the Betic Cordillera, along with the deep distribution of the allochthonous bodies emplaced on the southern border of the basin and the geometry of the External Zones.

2. Geodynamic Setting

[6] The Iberian Peninsula (Figure 1) was deformed mostly during Variscan orogeny, and, to a lesser

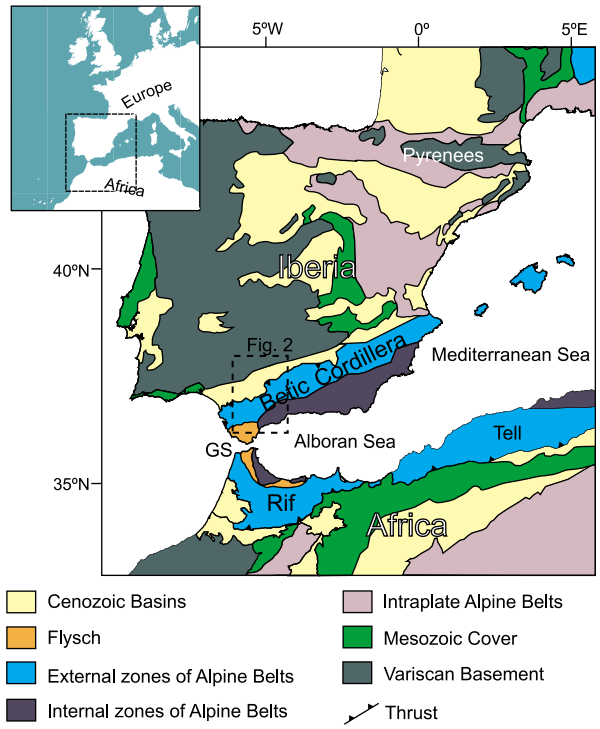

Figure 1. Geological setting. (left) General location of the Iberian Peninsula. (right) Enlarged geological map of the study area in the context of the western Mediterranean.

extent, during Alpine orogeny. The Iberian Massif is the largest continuous outcrop of the Late Paleozoic Variscan Orogen in western Europe. The Betic Cordillera was formed to the south of the Iberian Massif during Alpine orogeny by simultaneous westward migration and deformation of its internal zones within the general N-S to NW-SE oriented African-Eurasian plate convergence in the western Mediterranean. The External Zones of the Cordillera constituted the cover of the South Iberian paleomargin, deformed during intracontinental collision in the Early Miocene, forming a thin-skinned fold-and-thrust belt of sedimentary non-metamorphosed rocks [*Sanz de Galdeano and Vera*, 1992; *Lonergan and White*, 1997]. The Internal Zones consist of three main stacked metamorphic complexes and several frontal imbricated units that mainly outcrop in the western and central Betics. In the Early Middle Miocene, the Guadalquivir foreland Basin started to form toward the frontal part of the Cordillera associated with the progressive flexure of the Iberian Massif. Coevally, the Internal Zones were subjected to intense extensional process accommodated by detachments that culminated in the Alboran Basin development. Intramontane basins were progressively individualized at the edge of the large Alboran Basin as a result of eustatic and tectonic processes since the Late Miocene [*Sanz de Galdeano and Vera*, 1992].

3. Main Tectonic Complexes

3.1. SW Iberian Massif Foreland

[7] The Ossa-Morena and South Portuguese Zones (Figure 2) constitute the southern branch of the Iberian Massif defined by NW-SE trends and a SW regional vergence. The former belongs to the internal zones of the Variscan orogen and comprises Precambrian to Devonian pre-orogenic rocks affected by Late Palaeozoic metamorphism and ductile deformation [*Simancas et al.*, 2001]. The South Portuguese Zone is a Variscan foreland with Devonian and Carboniferous rocks affected by folds and thrusts [*Oliveira*, 1990]. The boundary between the two zones is interpreted as a suture corresponding to an oceanic domain [*Munhá et al.*, 1986].

3.2. External Zones (South Iberian Domain)

[8] Most of the profiles (Figure 2) traverse along the outcrops of the NE-SW to ENE-WSW thin-skinned fold-and-thrust belt constituted by the External Zones of the Betic Cordillera [*Sanz de Galdeano and Vera*, 1992]. The External Zones have been differentiated into the Prebetic and Subbetic domains [*Fallot*, 1948]. The Prebetic outcrops eastward of the study area, and is characterized by a typical imbricate thrust system of para-autochthonous shallow-water carbonate facies with terrigenous continental deposits [*García-Hernández et al.*, 1980]. The Subbetic is constituted by allocthonous pelagic units detached from its Variscan basement and was folded and thrusted under a nearly uniform WNW-NW transport direction during Early to Middle Miocene [*Pedrera et al.*, 2012]. It may be subdivided into External, Median and Internal zones on the basis of paleogeographic criteria. Accretion styles vary between the well-structured Internal Subbetics and the more complex Median and External Subbetics [*Pedrera et al.*, 2012]. The accretion process induced the extrusion of a synorogenic viscous tectonic mélange mainly constituted by Triassic clays and evaporites, also including carbonate and marly Jurassic, Cretaceous, and Tertiary rocks. In addition, Langhian to Early Serravallian olistostromic mass-transport deposits are particularly well developed in some sectors, mainly formed by components

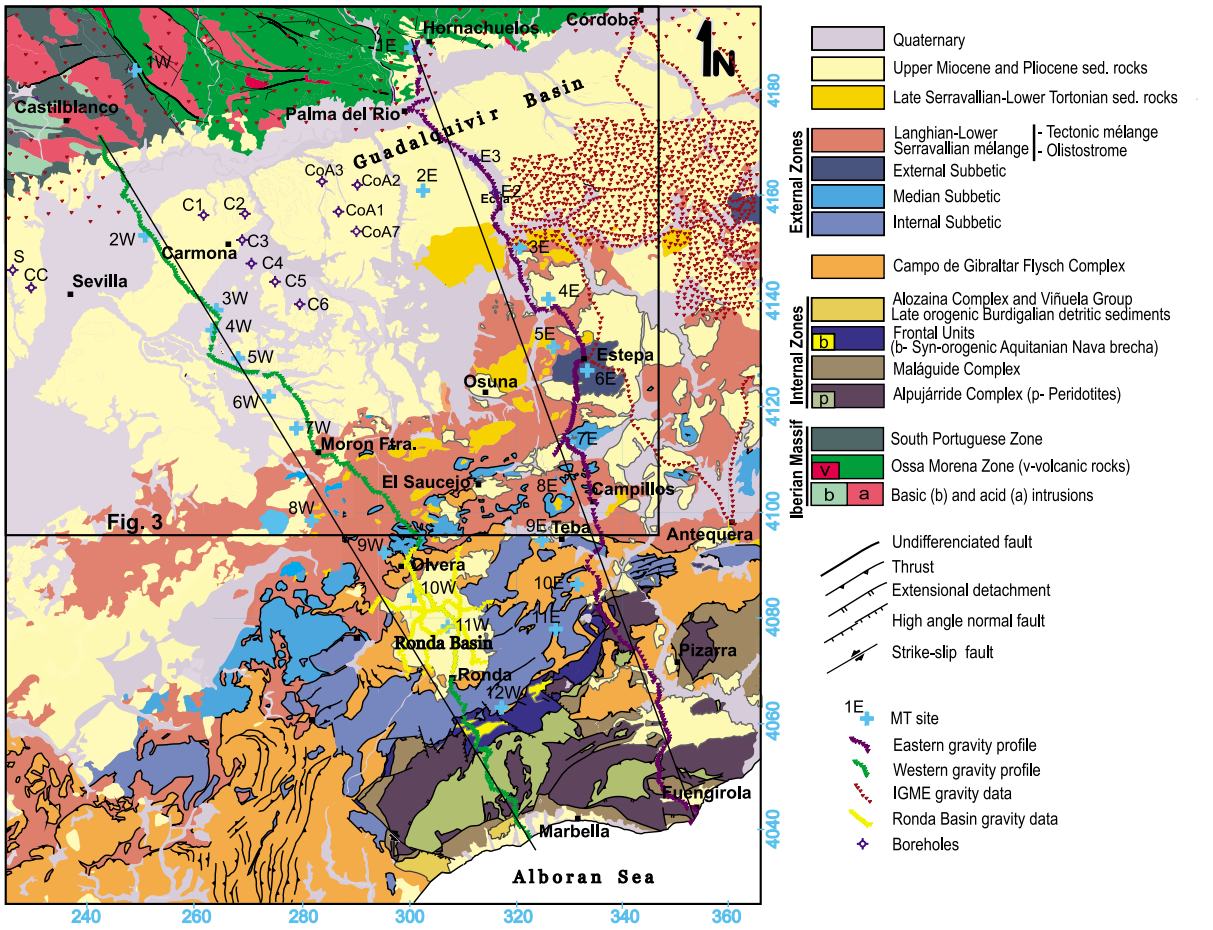

Figure 2. Geological map of the central-western Betic Cordillera with the location of the MT profiles, soundings and gravity stations; UTM coordinates, zone 30S.

derived from the previously described synorogenic tectonic mélange [*Roldán et al.*, 2012]. In the literature, the name and the processed involved in the formation of these chaotic units has been source of controversy [*Staub*, 1934; *Cruz-San Julián*, 1974; *Pérez López and Sanz de Galdeano*, 1994; *Roldán García*, 1995; *Berástegui et al.*, 1998; *Vera*, 2004; *Roldán et al.*, 2012]. In an attempt to unify definitions, we will refer to this unit as the frontal mélange unit [*Pedrera et al.*, 2012].

3.3. Flysch

[9] The Flysch units (Figure 2) are comprised of a stack of nappes, consisting of siliciclastic sediments of Cretaceous to Early Miocene age, not affected by Alpine metamorphism. They were deposited in an attenuated continental lithospheric setting, probably also including oceanic crust [*Durand-Delga et al.*, 2000]. The westward motion of the Internal Zones produced subduction of the oceanic floor and the deformation and emplacement of the Flysch Trough during the Early Miocene. Therefore, it constitutes an inactive accretionary prism that outcrops in the western Betics [*Luján et al.*, 2003], and extends between Ronda and Granada along the Internal/External Zone boundary.

3.4. Internal Zones (Alboran Domain)

[10] The Internal Zones (Figure 2) consist of several frontal imbricated units that mainly outcrop in the western and central Betics, in addition to three main stacked metamorphic complexes: in ascending order, the Nevado-Filábride, Alpujárride and Maláguide. The Maláguide is only weakly affected by Alpine metamorphism [*Chalouan and Michard*, 1990; *Lonergan*, 1993], whereas the two lower complexes record intense polyphase deformation including Alpine high-pressure metamorphism [*Tubía et al.*, 1992; *Azañón et al.*, 1997; *Balanyá et al.*, 1997]. A thick slice of peridotites from the lithospheric mantle and associated mafic rocks also outcrop in the Alpujárride Complex [e.g., *Mazzoli and Algarra*, 2011].

3.5. Neogene Basins

[11] The Neogene Guadalquivir foreland Basin (Figure 2) has an asymmetric geometry controlled by the lithospheric flexure of the Variscan basement as consequence of crustal thickening of the Betic Cordillera since Middle Miocene times, in the context of the Eurasia-Africa plate convergence. The depositional sequences outcropping at its northern boundary comprise autochthonous sediments (Late Tortonian-Pliocene) that unconformably overlie the Iberian Massif [*Roldán García*, 1995]. In contrast, those outcropping at the southern border (Late Langhian-Late Tortonian) are highly deformed and have been considered as allocthonous.

[12] The main Neogene intramontane basin of the western Betic Cordillera is the Ronda Basin. It is located at the boundary between the Internal Subbetic units —to the south— and the Flysch and mélange to the north. The sedimentary sequence of the basin is mainly formed by Late Miocene calcarenites and marls [*Serrano*, 1979].

4. Previous Geophysical Research

4.1. Seismic Data

[13] Deep seismic studies carried out in the southern Iberian Massif established the Moho depth at around 33–34 km [*Córdoba et al.*, 1988; *Suriñach and Vegas*, 1988; *Banda et al.*, 1993]. In the Betic Cordillera, the greatest crustal thickness (37–38 km) is reached below the large-scale kilometer-sized folds of the Internal Zones, and decreases to 23–25 km along the south and southeast coast of the Iberian peninsula — except in the area close to the Gibraltar arc that is characterized by 28–31 km Moho depths [*Banda and Ansorge*, 1980; *Medialdea et al.*, 1986; *Barranco et al.*, 1990]. Also present are crustal detachment levels that probably separate the upper crust, corresponding to outcropping rocks, from the lower crust [*Banda and Ansorge*, 1980; *Banda et al.*, 1993; *Galindo-Zaldívar et al.*, 1997]. In the western Betics, it is probably related to a detachment surface that separates, respectively at 10 and 12 km, the Iberian Massif basement from the External and Internal Zones [*Carbonell et al.*, 1998]. Below the Alboran Sea, the continental crust becomes thinner, to a minimum of 16 km in its central part [*Working Group for Deep Seismic Sounding in Alboran 1974*, 1978; *Torné and Banda*, 1992]. The low P and S velocities observed in the upper mantle of the Alboran Sea [*Banda et al.*, 1983], together with the high regional heat flow values [*Polyak*, 1996], suggest the existence of an anomalous mantle in this region [*Torné and Banda*, 1992; *Galindo-Zaldívar et al.*, 1998].

4.2. Magnetotelluric Data

[14] Magnetotelluric (MT) surveys previously undertaken in the southern Iberian Massif revealed the presence in the upper crust of high resistivity bodies related to Paleozoic series of rocks and to some unexposed plutons [*Pous et al.*, 2004]. In the lower crust, the main feature is a highly conductive zone in the Ossa Morena Zone that has been related to granulitic basement rocks with the presence of interconnected graphite [*Monteiro Santos et al.*, 1999; *Pous et al.*, 2004; *Almeida et al.*, 2005]. Other mid-crustal conductive bodies correlated with the main thrust zones formed during Variscan shearing processes [*Monteiro Santos et al.*, 2002], as the contact between the South Portuguese and Ossa Morena Zones [*Almeida et al.*, 2001]. In the Betic Cordillera, MT studies have been traditionally focused on the crustal structure of its more active eastern part [*Pous et al.*, 1999; *Martí et al.*, 2009; *Pedrera et al.*, 2009, 2010], while west of the 4°W meridian they are scarce and mainly address the lithospheric structure and its implications for geodynamic models [*Ruiz-Constán et al.*, 2010; *Rosell et al.*, 2011].

4.3. Gravity Data

[15] The Instituto Geográfico Nacional (IGN) gathered the gravity data used to construct the 1:1.000.000 free air and Bouguer anomaly maps [*Instituto Geográfico Nacional* (*IGN*), 1976] available for the Iberian Peninsula. In the study region, the Bouguer anomaly approaches zero values close to the northern boundary of the Guadalquivir Basin. To the north, the SW Iberian Massif gravity data reveal a NE–SW gradient, with values near zero in the Ossa Morena Zone and positive values in the South Portuguese Zone. In this setting, a constant Moho depth of around 33–34 km has been proposed for both domains [*Sánchez Jiménez*, 2004]. The Betic Cordillera is associated with a gravity minimum, which extends from the Gulf of Cadiz to the Balearic Islands, due to regional thickening of the crust and the local presence of low density sediments. The crust thins from 32–38 km below the Internal Zones to 15–22 km beneath the Alboran Sea, depending on the transect analyzed [*Torné and Banda*, 1992]. Positive values detected along the Málaga coast are related to the presence of Ronda peridotites [*Bonini et al.*, 1973]. However, the anomaly is placed southward of the peridotitic outcrops, pointing to the existence of deeper basic

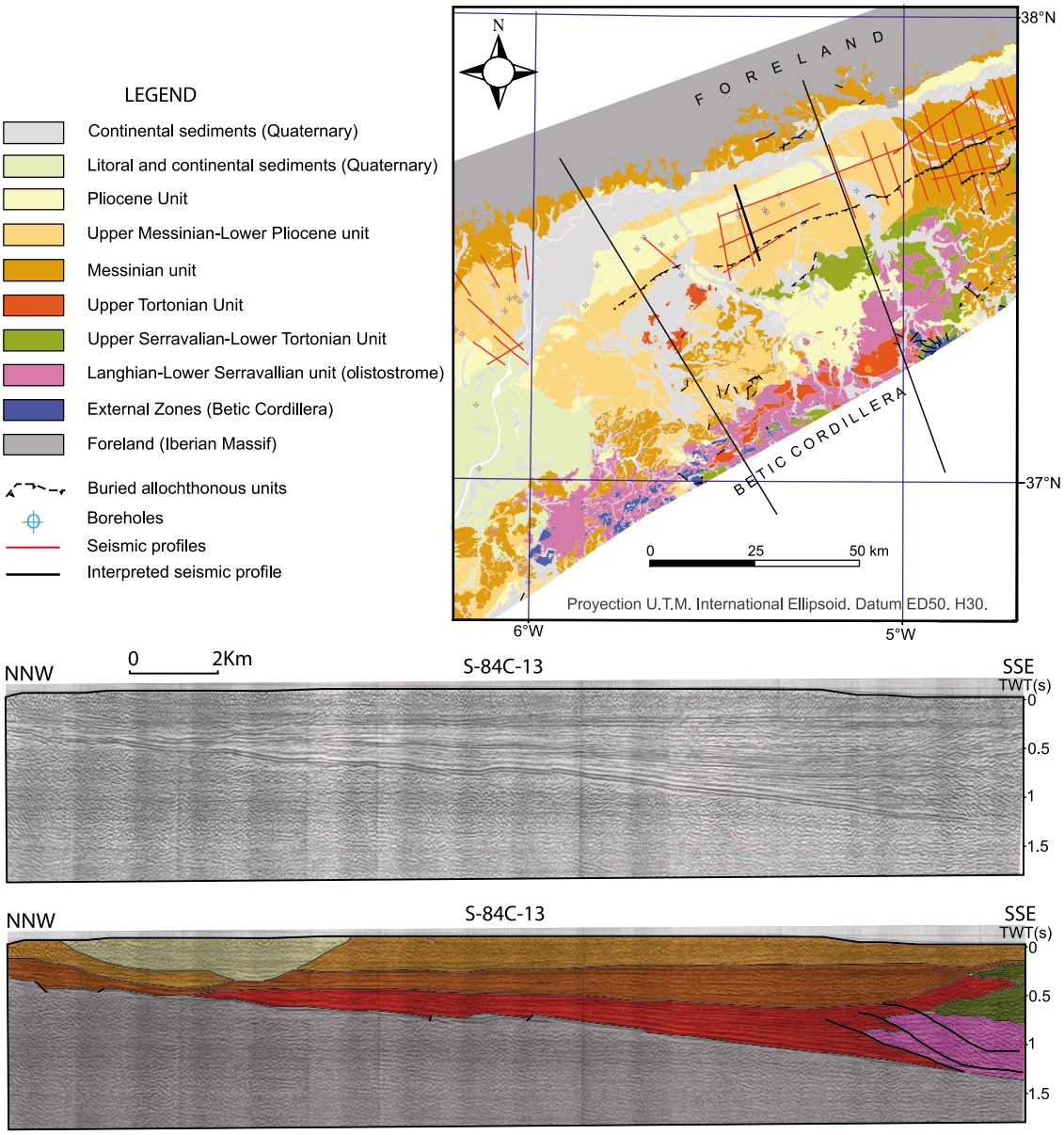

Figure 3. (top) Detailed map and (bottom) S-84C-13 seismic profile (IGME http://www.igme.es/internet/sigeof/inicio_spa.html) of the Guadalquivir basin sedimentary infill.

bodies [*Torné et al.*, 1992]. From the coast toward the Alboran Sea, the gravity values show a steeper increase [*Casas and Carbó*, 1990], revealing the southward thinning of the crust [*Torné and Banda*, 1992].

5. Borehole and Seismic Reflection Data in the Guadalquivir Foreland Basin

[16] The sedimentary sequence of the Guadalquivir Basin has been extensively studied through boreholes [*Instituto Geológico y Minero de España* (*IGME*), 1987] and seismic reflection profiles [*Roldán García*, 1995] acquired by oil exploration companies (Figure 3). These profiles (e.g., S84C-13 in Figure 3) image the geometry of the top of the basement and the sedimentary sequence of the Guadalquivir basin. At the southern boundary, the Upper Tortonian unit is overlied by the Langhian-Lower Serravallian and the Upper Serravallian-Lower Tortonian units at medium levels of the series. Meanwhile, the upper part of the series seals both units. The Messinian and Upper Messinian-Pliocene rocks onlap onto the foreland, meanwhile

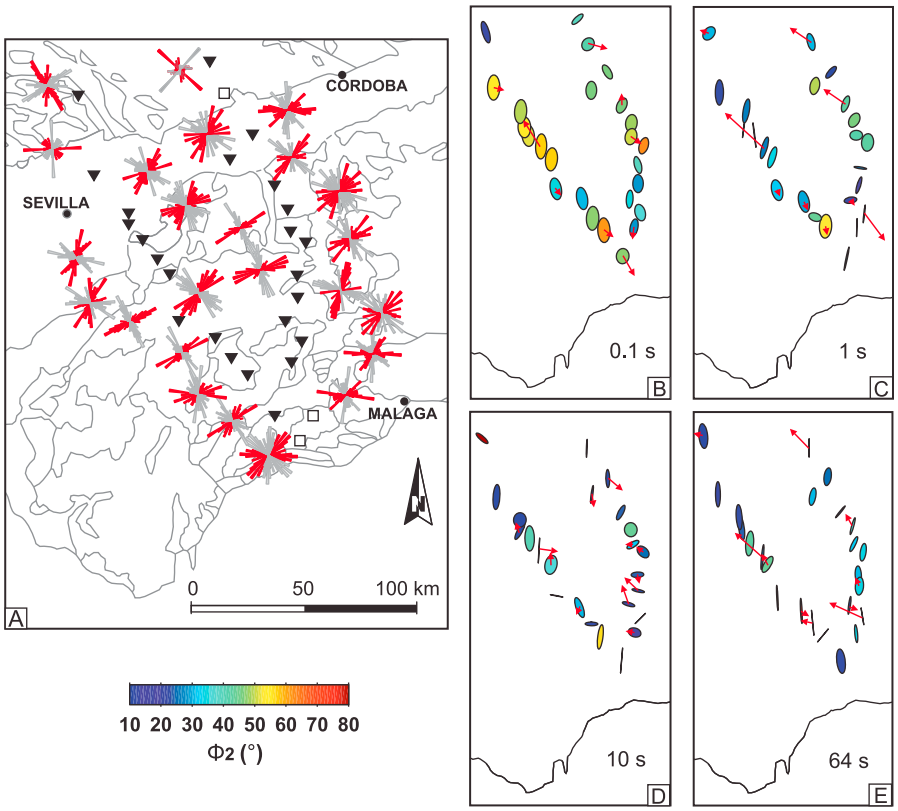

Figure 4. Dimensionality analysis of the MT data. (a) Rose diagrams of the phase consistent strike results including all periods for the sites inverted in the 2D model (triangles). Squares are the sites not included in the 2D inversion. (b–e) Phase tensor and induction arrow sections at different periods.

the Pliocene unit is restricted to the northern part of the profile.

[17] In addition, logs from 13 commercial boreholes (Figures 2 and 8) were selected in order to constrain the geophysical models. Seven of them (S, CC, C1, CoA1, CoA2 and CoA3; Figure 2) cross the sedimentary infill overlying the Iberian Massif, showing increasing depth of the basement toward the hinterland. Boreholes situated to the south (C2, C3, C4, C5, C6 and E2) also go through sediments involved in the mélange, at a maximum depth of approximately 1.8 km in C6. However, since the imaging of plastic units (clays, gypsum…) is usually problematic using seismic techniques, given the occurrence of energy-absorption problems that mask the deeper structure, southward of the Guadalquivir Basin it is necessary to combine this results with information provide by other geophysical data.

6. New Magnetotelluric Data

[18] New broadband magnetotelluric data were acquired along two transects of the western Betic Cordillera, from the Iberian Massif foreland to frontal units of the Internal Zones of the Cordillera (Figure 2). Magnetotelluric (MT) results allow us to characterize the electrical structure of the upper crust and provide information on the geometry and depth of the Iberian Massif below the western Betic Cordillera and the structure of the Betic External Zones.

6.1. Data and Methodology

[19] The MT technique is an electromagnetic (EM) method used to constrain spatial variations of the Earth's resistivity by measuring, simultaneously, the natural time-varying electric and magnetic fields at the Earth's surface in orthogonal directions [*Vozoff*, 1972]. The components of the EM field were measured using Metronix ADU06 equipment, covering a period band from 0.001 to 100 s. The survey consists of 23 magnetotelluric sites along two profiles approximately orthogonal to the main geological trend of the Betic Cordillera. Spacing between sites was around 5–15 km. The western profile (Profile 1; Figures 2 and 4) comprised twelve sites placed in a NW–SE direction along ~130 km

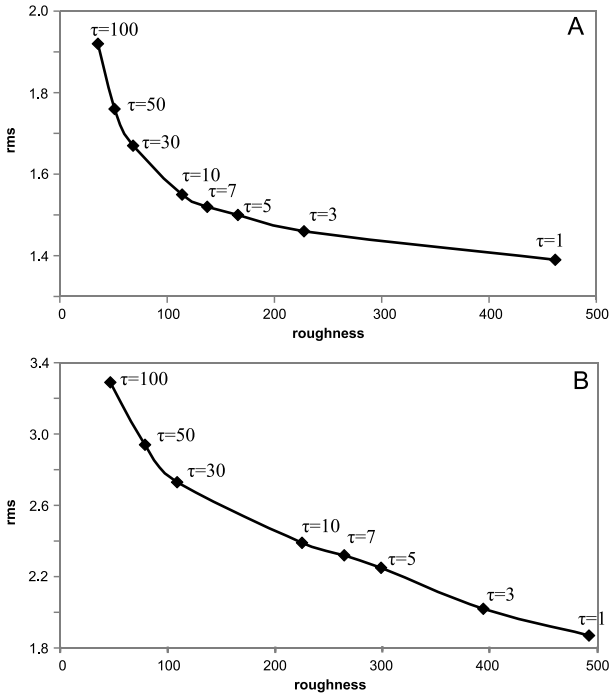

Figure 5. L curve, trade-off between model roughness and root mean square (rms) of the (a) western and (b) eastern profile models.

between the cities of Marbella and Castilblanco. The easternmost profile (Profile 2; Figures 2 and 4) comprised eleven sites in a NNW–SSE direction along ∼120 km from Fuengirola to Hornachuelos. The space between sites is greater in the northern part of the profiles because this area is crossed by railway lines and high-voltage power lines that both produce EM noise. In addition, the southern extension of both profiles is compromised by the highly populated villages along the Malaga coast. The time series were processed using a standard robust processing algorithm [*Egbert and Booker*, 1986] to obtain the impedance tensor components. The data finally used in the analysis were generally of good quality, which decreases considerably between 10 and 100 s (Figure 6).

6.2. Dimensionality Analysis

[20] The dimensionality analysis was performed using two approaches: Bahr decomposition [*Bahr*, 1988, 1991] and phase tensor analysis [*Caldwell et al.*, 2004]. The determination of the strike direction has an inherent ambiguity of 90° because, when axes are rotated to achieve an ideal two dimensional medium, there is no a priori indication from the MT data about which axis direction is along strike and which is orthogonal to it. This ambiguity was solved considering the known strike direction of the main geological contacts together with the real induction arrows (Figure 4) that are commonly sensitive to lateral electrical resistivity variations, pointing toward the conductive zones [*Parkinson*, 1962]. Figure 4a shows the results from Bahr decomposition for each MT station. The rose diagrams show a homogeneous geoelectrical strike, giving a general NE–SW to ENE–WSW direction (Figure 4b) at the Betic Cordillera sites for periods shorter than 100 s. These directions are in agreement with those calculated by *Rosell et al.* [2011]. However, a more heterogeneous pattern was observed at longer periods due to the generalized change in the geoelectrical strike to a N–S direction below 100 s [*Ruiz-Constán et al.*, 2010]. The change in strike trend defined the period range, inverted to periods lower than 100 s. Thus, for 2D inversion purposes, a geoelectrical strike of N55°E was chosen.

[21] The phase tensor (Φ) can be depicted graphically as an ellipse, the major (Φ_{max}) and minor (Φ_{min}) axes representing the principal axes of the tensor. The color used to fill the ellipses represents the geometric mean of the maximum and minimum phase (Φ_2), high values being indicative of increasing conductivity with depth. In the study area (Figure 4), the direction of the phase tensor principal axis is also consistent with the strike found while the high Φ_2 values indicate the location of anomalous conductive zones in the frontal and shallow parts of the cordillera.

6.3. 2D Inversion

[22] A joint 2D inversion [*Rodi and Mackie*, 2001], of 55° rotated apparent resistivities and phases, was carried out. The tipper was not included in the inversion due to some problems appeared in the vertical magnetic component that resulted in a low quality tipper data. Static-shift effects were detected as displacements between the TE (Transversal Electric Model) and TM (Transversal Magnetic Model) modes at the shortest periods of curves 9W and 6E. All the corrections were smaller than one decade. The model Fuengirola-Hornachuelos (eastern profile) minimizes second derivatives using a uniform grid Laplacian and a smoothing factor (τ) of 7. This value was determined through optimizing the tradeoff between the RMS misfit and the smoothing of the model (Figure 5a). An error floor of 8% for the apparent resistivities and 4% for the phases was used in the inversion for both modes. A number of inversions were carried out with different error floors around these values, always giving the

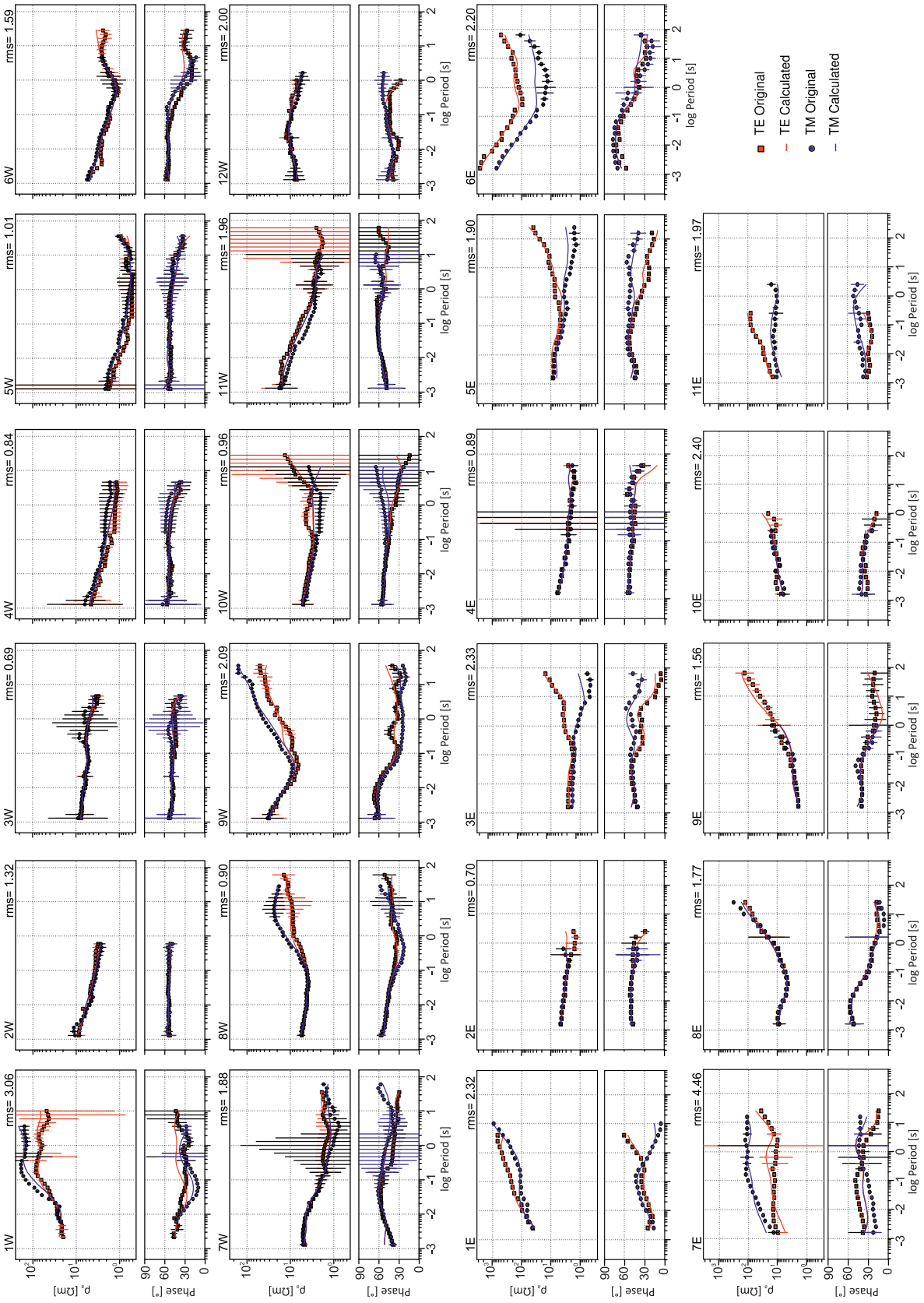

Figure 6. Data and model responses, apparent resistivities (ρ_a) and phases (red, TM mode; blue, TE mode).

same relevant features in the final inverse models. The best fitting model (RMS = 2.25) was obtained through the following pattern. First, the TM mode was inverted with a homogeneous intermediate resistivity of 100 Ohm·m and with a regular lateral cell size increasing with depth. Second, this inverse model result was used as an initial one for joint inversion of the TM mode and TE mode data simultaneously.

[23] The same procedure was undertaken for the western model (Figure 5b). The smoothing factor τ selected during inversion was 7, and the error floor considered for resistivity and phases of both polarization modes were 6% and 3%, respectively. The resistivity image obtained shows the lowest misfit achieved (RMS = 1.53) and the best geological correlation with the outcropping structures. Model responses for the profile 1 and profile 2 sites are shown in Figure 6. The difference pseudosections between the observed and modeled responses for all the sites along the profile show that generally a good fit is achieved for both the TE and the TM modes (Figure 7).

6.4. Geological Interpretation of Resistivity Data

[24] Figure 8 shows the results of the two inversion models which, at first glance, reveal the same main features. The northwestern edges are characterized by an almost continuous resistive layer extending considerably in depth to the SE below a more heterogeneous upper crust. This geometry confirms the continuity in depth of the Iberian Massif below the Guadalquivir foreland basin and the External Zones of the Betic Cordillera. The absolute electrical conductivity of this layer is fairly homogeneous. However, the great thickness of the conductive bodies located below sites 4E-7E and 4W-8W mask their continuity in this part of the profiles. Hypothesis testing showed that the resistivity of this area is only weakly resolved by the data. A wedge-shaped high conductive body (~3–15 Ohm·m) is located in the shallow part of the models between sites 2W-8W (western profile) and 2E-6E (eastern profile). It correlates with Neogene sediments of the Guadalquivir foreland basin and the frontal mélange unit. Its thickness increases from north to south until reaching ~5 km, although its geometry is more irregular and discontinuous on the eastern profile.

[25] At stations 5E, several relatively resistive bodies (~500 Ohm·m) appear below the southern border of the wedge, finally outcropping at sites 6E and 7E. They are also observed below sites 8W to 10W. These resistive zones correlate well with the locations of bodies formed by Subbetic carbonates. In the shallow part, the same lithology seems to have enhanced conductivity, probably reflecting the presence of saline water in these highly permeable rocks. Between sites 10W and 11W, a conductive zone (~4–15 Ohm·m) coincides with the sedimentary infill of the Ronda Basin, the clays and gypsum matrix of the frontal mélange and a chaotic unit mainly involving Flysch, both constituting the basement of the northern part of the sedimentary infill. The continuity of the Iberian massif below the External Zones at the southern end of the profile is masked due to their similar resistivity values. The models will be described and interpreted in detail in light of the geological cross-sections and information provided by the seismic profiles, borehole and gravity data (see section 8).

7. Gravity Data

7.1. Methodology and Acquisition of New Gravity Data

[26] New gravity data (Figure 9) were acquired along the MT transects, reaching southward as far as the coastline. They were complemented with additional data from the Instituto Geológico de España database (IGME, http://www.igme.es/internet/sigeof/inicio_spa.html) and from a detailed survey in the Ronda Depression [*Ruiz-Constán et al.*, 2009]. Altogether, these data help to corroborate the crustal structure established by the resistivity image, and propose its southward continuity.

[27] The eastern and western profiles respectively comprise 348 and 338 gravity stations. Mean spacing between stations is 500 m. The data were acquired using a CG-5 Scintrex gravimeter with a maximum accuracy of 0.001 mGal that automatically corrects for instrument drift and tidal variations. The measurement stations were positioned with an e-trex Garmin GPS and a barometric altimeter with 0.5 m altitude precision. The absolute altitude of the stations was established through measurements in several geodetic references near the profile. In order to determine the absolute gravity value, data were calibrated to the Málaga and Sevilla base stations of the IGN national gravimetric network. Topographic correction was performed up to a distance of 22 km using a digital terrain model with a grid of 90 m cell size due to the limited effect of the farthest reliefs. The Bouguer

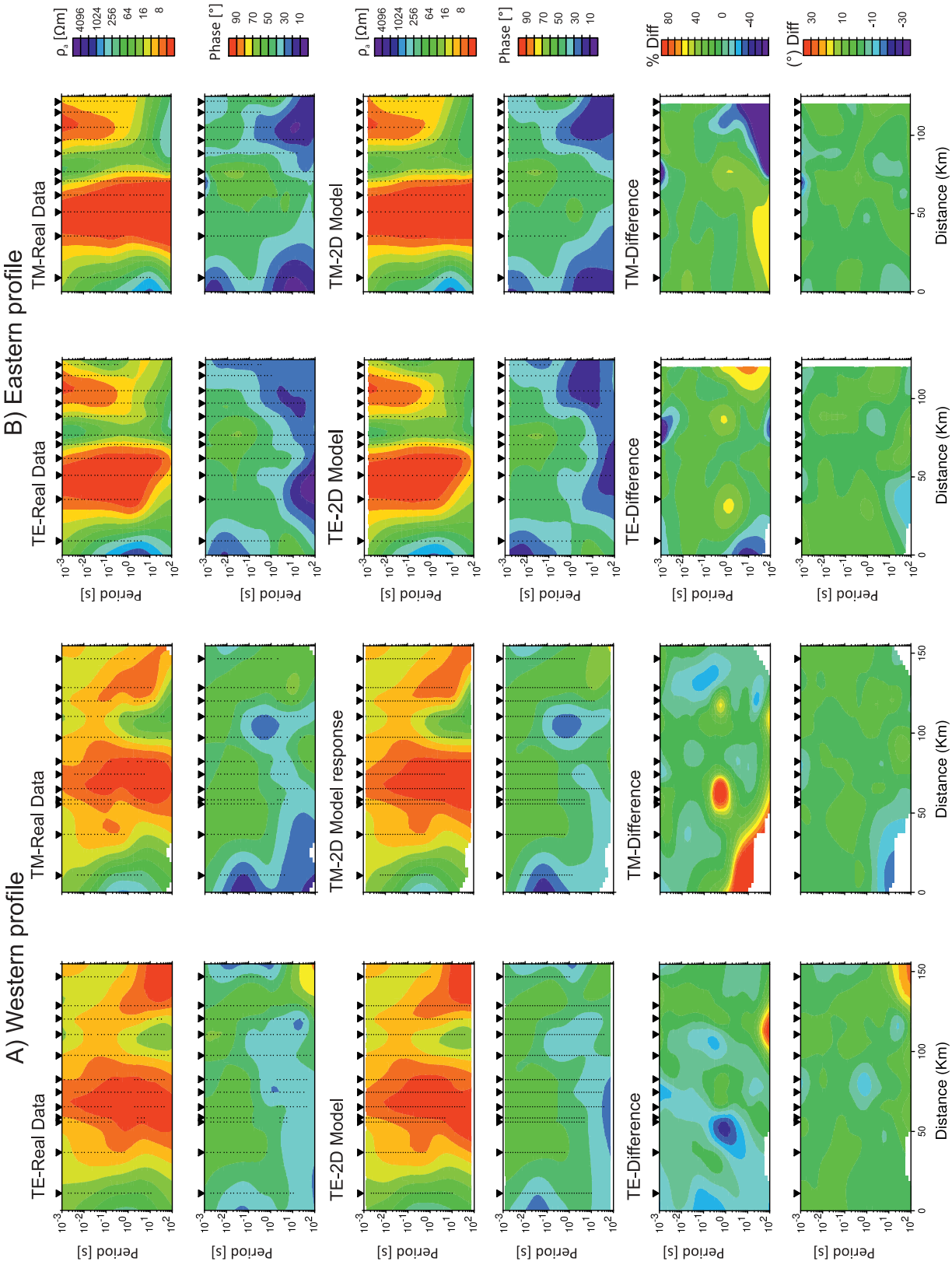
A) Western profile
B) Eastern profile
TE-Real Data
TM-Real Data
TE-2D Model
TM-2D Model response
TM-2D Model
TE-Difference
TM-Difference
Period [s]
Distance (Km)
ρa [Ωm]
Phase [°]
% Diff
(°) Diff

Figure 7

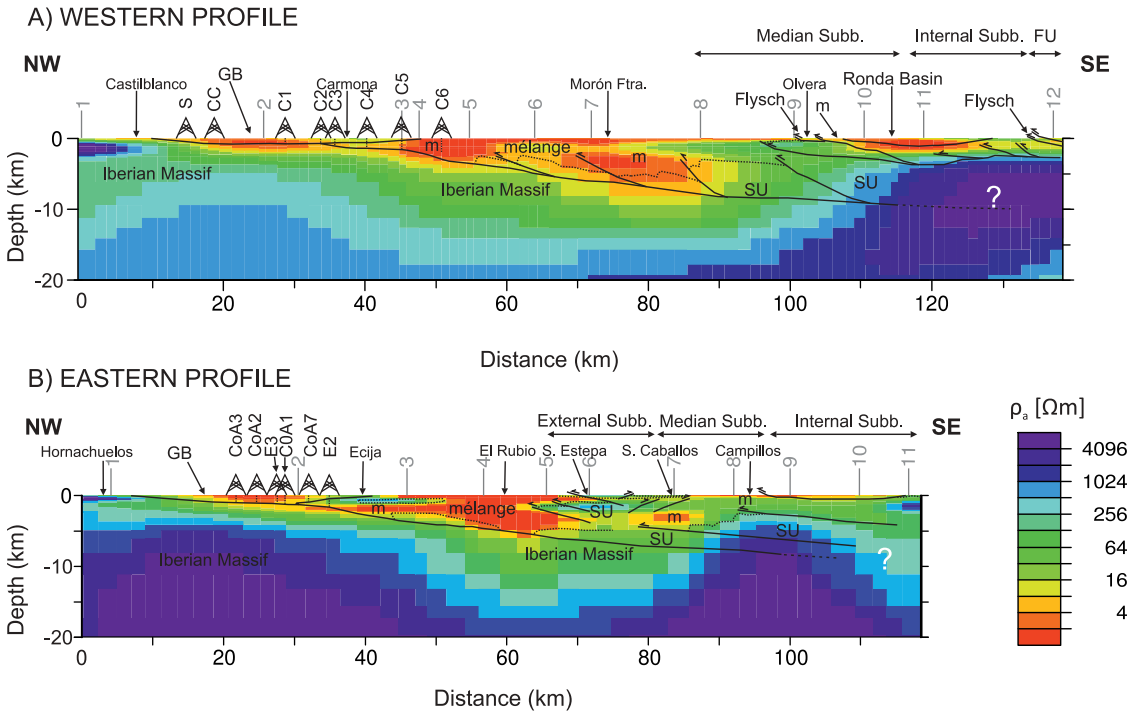

Figure 8. Two-dimensional electrical resistivity model along the MT profiles with indication of the main highly resistive and highly conductive zones and geological structures discussed in the text. FU, Frontal Units of the internal Zones; GB, Guadalquivir Basin; m, mélange; SU, Subbetic Units; the location of the MT sites and the boreholes in Figure 3 are marked.

anomaly was calculated taking into account a standard density of 2.6 g/cm^3.

7.2. Gravity Modeling and Crustal Structure

[28] The study of the Bouguer gravity anomaly in complex tectonic areas, where many bodies contribute to the anomaly, implies that gravity models are not unique and diverse proposals could give similar model responses. Therefore, previous data on the geological surface structure, boreholes, seismic and magnetotelluric profiles are needed to better constrain realistic models. We propose two new 2.5D NW-SE gravity models developed using the GRAVMAG V.1.7. software of the British Geological Survey [*Pedley et al.*, 1993] that integrate the new 2D resistivity models and previous geological and geophysical data [*Medialdea et al.*, 1986; *IGME*, 1987; *Morales et al.*, 1999]. The average density assigned to each geological unit is related to its main lithology according to standard values [*Telford et al.*, 1990] and previous studies in the area [*Sánchez Jiménez*, 2004].

[29] The gravity profile (Figure 10) shows the transition from the stable continental crust of the Iberian Massif through the cross-section of the Betic Cordillera, up to the thinned continental crust of the Alboran Sea margin. The positive Bouguer anomaly values toward the northwestern end of the profile infer the presence of a high density body, possibly basic rocks, that extends northward beyond the profile and is probably located at middle levels of the Iberian crust [*Sánchez Jiménez*, 2004]. The high anomaly values, reaching 80 mGal, are determined by the presence of this body and are not observed to the east or west of this profile [*IGN*, 1976]. To the south, the Iberian Massif continues below the Betic Cordillera, and a decrease in the Bouguer anomaly is produced by the low density Neogene sediments of the Guadalquivir and Ronda Basins and the Mesozoic-Cenozoic sedimentary rocks of the External Zones of the Betic Cordillera.

Figure 7. Magnetotelluric pseudosections. Apparent resistivity and phase pseudo-sections of the two MT profiles, for both the observed and modeled responses, as well as difference pseudo-section between the observed and modeled responses. The difference pseudo-section clarifies the spatial areas and period ranges that are well fit and poorly fit in the model.

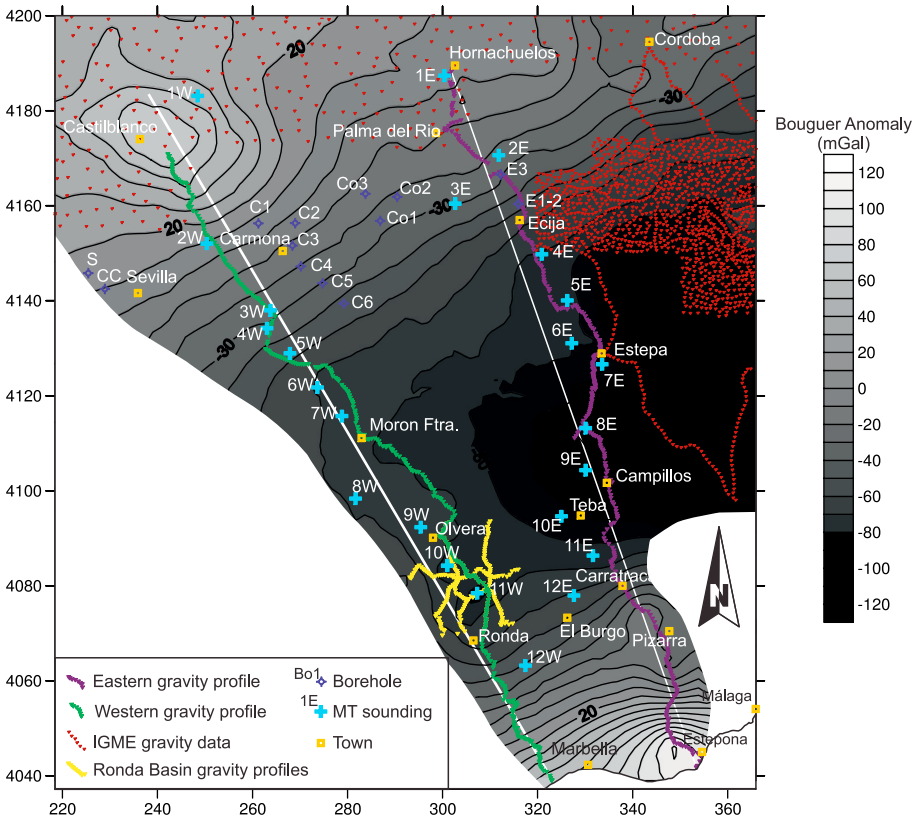

Figure 9. Bouguer gravity anomaly map integrating all the available data; UTM coordinates, zone 30S.

[30] From the stable Iberian Massif, Moho depth increases southwards below the Guadalquivir Basin and the External Zones due to the load of the Betic Cordillera. Southwards, Iberian continental crust sinks into the mantle toward the Alboran Sea, as corroborated by the seismicity distribution and available seismic tomography data [*Morales et al.*, 1999]. The overprinting of several bodies, like the continental crust sinking into a dense mantle, makes it difficult to accurately determine the deep structure of each one but they support the proposed deep structural model.

8. Discussion

[31] Figure 10 integrates all the available information in order to produce a regional image of the crust over the whole area. The upper part is well constrained and based on geological knowledge of the different complexes and their structural relationships. The structure at depth, while more speculative, is based on the MT 2D inversion models interpreted in terms of lithology and with other geophysical data (seismic profiles, borehole and gravity data). The use of different techniques assuages the limitations of each method. The MT survey was highly affected by electrical noise interference owing to anthropic activity along the Guadalquivir Basin and the cities along the coastline. This impeded the southward continuity of the resistivity model toward the coast, and necessitated the larger spacing of the soundings in its northern part. The southern continuation of both transects was constrained by the gravity models, whereas the northern part was constrained by the information provided by the seismic lines and borehole data. The high conductivity values obtained in the shallower part of the MT profiles also reduces resolution of resistivity structures below 20 km. The Moho depth is established in our model by previous seismic information [*Medialdea et al.*, 1986] and slightly modified by gravity anomaly data.

[32] In comparable examples, the dip of the foreland at the frontal part of the orogenic wedge and below the external thrusts ranges from low values of 1–5° to high values of 10–20° [*Davis et al.*, 1983; *Jaumé and Lillie*, 1988; *Talbot and Alavi*, 1996; *Ford*, 2004]. Similar variability is observed in the circum-Mediterranean belt, for example, by comparing the Alps and the Apennines. In the former, this angle varies from 2 to 3° at the front of the accretionary wedge to about 5° beneath the external

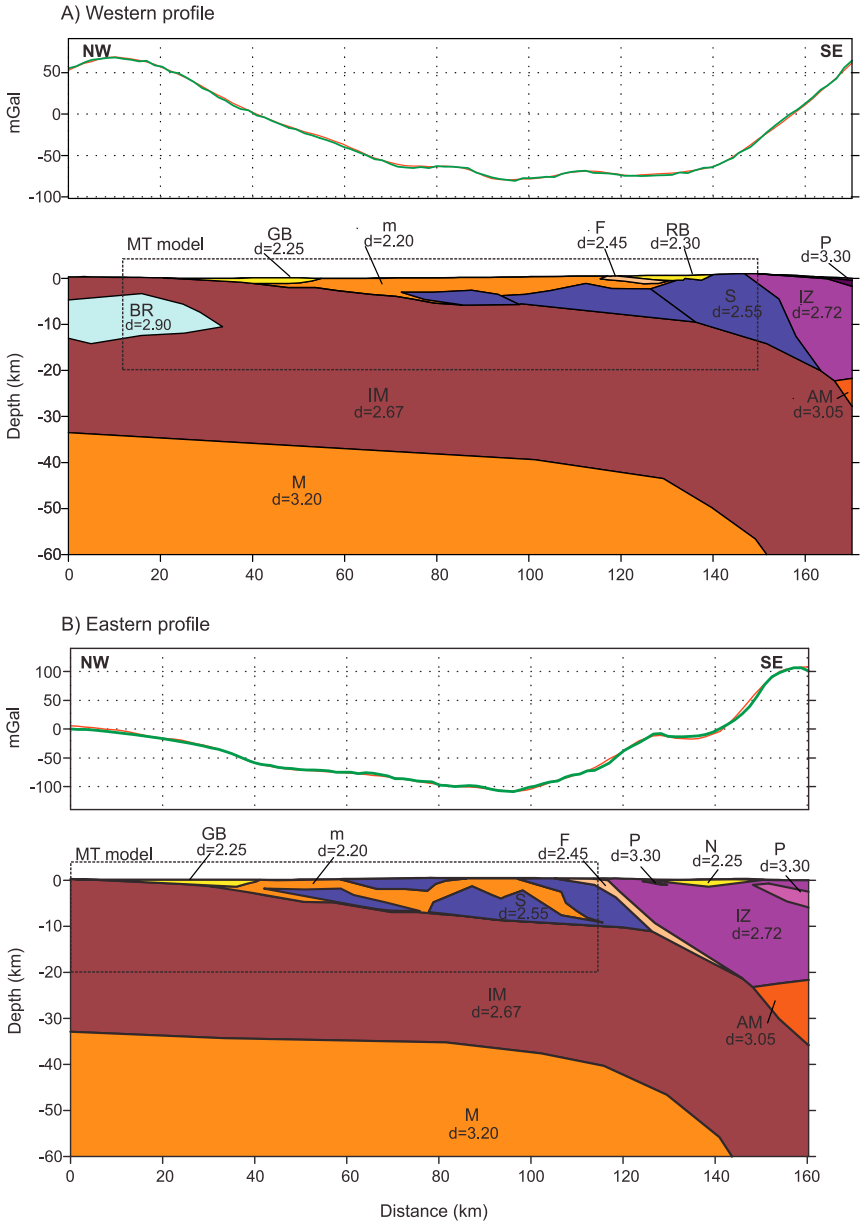

Figure 10. Gravity models. Densities are indicated in g/cm^3: AM, anomalous mantle; BR, basic rocks; GB, Guadalquivir Basin; F, Flysch, IM, Iberian Massif; IZ, Internal Zones; m, mélange; M, mantle; N, Neogene sediments; P, peridotites; RB, Ronda Basin; S, Subbetic.

thrusts. In the latter, the dip is higher and respectively varies from 4–5° to 10°, although there are areas where it exceeds 20° [*Mariotti and Doglioni*, 2000]. Boreholes and seismic lines show that the Iberian Massif, below the Guadalquivir basin and the External Zones, is tilted toward the SE with a slope increasing from 2.5° to 6° [*García-Castellanos et al.*, 2002] and reaches depths of 5 km at a distance of 60–80 km from the southern outcrops of basement [*Fernàndez et al.*, 1998]. Other geological cross-sections [*Crespo-Blanc and de Lamotte*, 2006] propose a uniform slope ranging from 6.5° in the central Betics (Jaen-Granada transect) to 5° in the western sector (Almonte-Manilva transects). The MT models for both profiles supports a nearly horizontal slope (2°) below the Guadalquivir basin, with the frontal part of the orogenic wedge increasing toward the SE and giving values between 6 and 8° below the External Zones (Figure 8). The basement top reaches depths of approximately 5–7 km at a distance of 60–80 km from the first foreland outcrops. However, these

values cannot be extrapolated to other transects of the Betic Cordillera, as lateral variation in the foreland dip angle has been widely described in tectonic arcs associated with lateral variations of the inherited crustal and lithospheric thicknesses and compositions [*Mariotti and Doglioni*, 2000].

[33] Several changes in the slope observed in the central part of both profiles could be related to normal faults that deform the basement top. The presence of these faults is reflected by seismic lines in the lower part of the Guadalquivir sedimentary infill [*Fernàndez et al.*, 1998] and could be a consequence of basement flexure. Toward the Internal Zones, gravity models support the notion that basement dip increases up to roughly 20–35° below the coastline, showing a curved geometry in depth. This geometry is in agreement with the context of the partial subduction of continental Iberian crust below the Alboran Sea, previously pointed out by seismic tomography [*Morales et al.*, 1999] and seismotectonic analysis of earthquake focal mechanisms [*Ruiz-Constán et al.*, 2011].

[34] The greatest thicknesses of the conductive rocks of the mélange unit are located above the frontal resistive bodies that correspond with the Jurassic and Cretaceous sequences of the External (eastern transect) and Median (western transect) Subbetics, pointing to the Subbetic provenance of these plastic rocks [*García-Dueñas*, 1969; *Sanz de Galdeano*, 1975; *Pedrera et al.*, 2012]. Below several Jurassic-Cretaceous Subbetic reliefs of the more frontal part (such as Sierra de Estepa; sites 6–7, eastern profile), the resistivity profile shows additional underlying repeated sequences of more resistive Subbetic sheets separated by the conductive mélange matrix bands (clays, sandstones and gypsum). Furthermore, the Subbetic of the Estepa range has a well-defined structure characterized by curved folds mainly developed above NW–WNW directed thrusts [*Pedrera et al.*, 2012]. These ranges, apparently chaotically placed within the mélange unit, were previously described as large isolated blocks floating over the plastic mélange. The bottom of the stacked carbonate sequences reaches around 8 km in depth below the external zones and is similar to the one proposed in other cross-sections of the Cordillera [*Banks and Warburton*, 1991; *Platt et al.*, 2003; *Crespo-Blanc and de Lamotte*, 2006]. However, on the basis of our resistivity models, we cannot discard a Prebetic provenance of the deeper high resistive rocks, given their lithological similarities, as pointed out in the western sector [*Flinch et al.*, 1996; *Platt et al.*, 2003].

[35] We hold that the extrusion of the plastic rocks that constitute the mélange matrix was aided by the load and compression linked to the progressive Subbetic units accretion. Accreted rocks, as a result of tectonic collision, were incorporated to a frontal prism including: Triassic clays, evaporites and ocean-floor basalts, Mesozoic and Neogene platform and pelagic sediments, and fragments of metamorphic rocks. Interplay of tectonic, gravitatory and diapiric processes configured the complex structure of this unit. *Berástegui et al.* [1998] considered that plastic rocks were originally placed below the Intermediate Units. However, the MT models reveal a Subbetic affinity, suggesting that their extrusion occurs in different places: at the front of the Internal Subbetic (conductors beneath Olvera and Campillos in Figure 8), at the front of the Median Subbetic (conductors beneath Sierra de los Caballos and Morón in Figure 8) and at the front of the External Subbetics (conductor north of Estepa, Figure 8). In addition, the models show that extruded plastic mélange cover, or "canopy," some stacked carbonate Subbetic sequences, and account for the continuity in depth of the resistive stacks of Jurassic limestones that outcrop in some ranges (e.g., the Estepa Range).

[36] The sequence of deformation and emplacement of the Subbetic ranges and the progressive frontal accretion of the mélange unit are interpreted as a continuous process linked to the Oligocene-Late Miocene E-directed subduction of oceanic crust and the thin continental crust of the Iberian margin beneath the Alboran continental Domain [*Pedrera et al.*, 2012]. In this context, our geophysical data suggest that the tectonic mélange, mainly formed by plastic Keuper Triassic evaporites, acted as the decoupling horizon facilitating a partial continental subduction of the Iberian continental crust. Although continental crust may be considered resistant to subduction due to its positive buoyancy, in certain convergence settings it may be at least partially subducted [*Chemenda et al.*, 1996; *Matte et al.*, 1997; *Faure et al.*, 2003]. As a broader approach, we propose that thick plastic rocks units placed above the foreland could act as a lubricant facilitating continental subduction, then being progressively accreted toward a frontal mélange.

9. Conclusions

[37] The MT method, which is highly sensitive to conductors, combined with gravity prospecting, sensitive to low density rocks, can accurately

characterize the subsurface structure of mélange units with a high content in wet evaporites and clays. This combined methodology is therefore the best option for imaging plastic units, since the use of seismic techniques is usually problematic given the poor continuity of reflectors and the occurrence of energy-absorption that usually mask the deeper structure. The derived MT and gravity models were also compared with geological information and complemented with further data, including seismic profiles and boreholes, to lead to a comprehensive interpretation of the deeper structure of two transects of the central and western Betic Cordillera.

[38] The main conductive bodies observed in the MT model are related to the claystones, sandstones and evaporitic rocks involved in the frontal mélange unit. The greatest thicknesses are located at the frontal part of the Cordillera. They overlie the Iberian Massif in the northern part and the frontal Jurassic and Cretaceous limestone sequences of the External and Median Subbetics toward the south. Internally coherent Subbetic units are less common toward the NW, where resistive bodies alternate with a greater amount of plastic rocks of the mélange matrix. Furthermore, there is continuity at depth of some Subbetic ranges previously described as large isolated blocks floating over the plastic mélange.

[39] Extrusion of the plastic rocks was favored by the load due to the progressive emplacement of the External Zones. Rocks of very different provenance were accreted as a result of tectonic collision, with the greatest thicknesses of plastic rocks located at the frontal part of the different Subbetic Units. The bottom of the stacked carbonate sequences reaches around 8 km depth below the External Zones and seems to be of Subbetic provenance, although the presence of Prebetic units cannot be discarded, given their lithological (and resistivity) similarities.

[40] The MT models show the continuity of the Iberian Massif foreland below the Betic Cordillera, with a nearly horizontal slope below the Guadalquivir foreland basin that increases toward the SE, reaching 6–8° below the External Zones. Several steps in the top of the resistive body, corresponding to the Iberian Massif foreland, could be related to the presence of normal faults deforming the basement. To the south, gravity models and earthquake distribution support the slope increasing up to approximately 20–35° below the Internal Zones and the Alboran coast, with a curved geometry. Our geophysical data suggest that the tectonic mélange, mainly formed by plastic Keuper Triassic evaporites, acted as the decoupling horizon facilitating a partial continental subduction of the Iberian continental crust. Although continental crust may be considered resistant to subduction, thick plastic rock units placed above the foreland could act as a lubricant facilitating the process, being progressively accreted toward a frontal mélange.

Acknowledgments

[41] This study was supported by the projects TOPO-IBERIA CONSOLIDER INGENIO CSD2006–00041, CGL-2008-03474-E, CGL2010–21048 and CGL 2008 0367 E/BTE of the Spanish Ministry of Science and Education, as well as by Research Group RNM-148 and RNM-5388 of the Junta de Andalucía Regional Government. We are sincerely grateful to Thorsten Becker, editor of G-Cubed, Whitney Behr and two anonymous reviewers for their constructive criticism of the paper.

References

Almeida, E., J. Pous, F. Monteiro Santos, P. Fonseca, A. Marcuello, P. Queralt, R. Nolasco, and L. Mendes-Victor (2001), Electromagnetic imaging of a transpressional tectonics in SW Iberia, *Geophys. Res. Lett.*, *28*(3), 439–442, doi:10.1029/2000GL012037.

Almeida, E., F. M. Santos, A. Mateus, W. Heise, and J. Pous (2005), Magnetotelluric measurements in SW Iberia: New data for the Variscan crustal structures, *Geophys. Res. Lett.*, *32*, L08312, doi:10.1029/2005GL022596.

Azañón, J. M., A. Crespo Blanc, and V. García-Dueñas (1997), Continental collision, crustal thinning and nappe forming during the pre-Miocene evolution of the Alpujarride Complex (Alboran Domain, Betic), *J. Struct. Geol.*, *19*(8), 1055–1071, doi:10.1016/S0191-8141(97)00031-X.

Bahr, K. (1988), Interpretation of the magnetotelluric impedance tensor: Regional induction and local telluric distortion, *J. Geophys.*, *62*(2), 119–127.

Bahr, K. (1991), Geological noise in magnetotelluric data: A classification of distortion types, *Phys. Earth Planet. Inter.*, *66*(1–2), 24–38, doi:10.1016/0031-9201(91)90101-M.

Balanyá, J. C., V. García-Dueñas, and J. M. Azañón (1997), Alternating contractional and extensional events in the Alpujarride nappes of the Alboran domain (Betics, Gibraltar Arc), *Tectonics*, *16*(2), 226–238, doi:10.1029/96TC03871.

Banda, E., and J. Ansorge (1980), Crustal structure under the central and eastern part of the Betic Cordillera, *Geophys. J. R. Astron. Soc.*, *63*, 515–532, doi:10.1111/j.1365-246X.1980.tb02635.x.

Banda, E., A. Udias, J. St. Mueller, M. Mezcua, J. Boloix, J. Gallart, and A. Aparicio (1983), Crustal structure beneath Spain from deep seismic sounding experiments, *Phys. Earth Planet. Inter.*, *31*, 277–280, doi:10.1016/0031-9201(83)90087-0.

Banda, E., J. Gallart, V. García-Dueñas, J. J. Dañobeitia, and J. Makris (1993), Lateral variation of the crust in the Iberian peninsula: New evidence from the Betic Cordillera, *Tectonophysics*, *221*, 53–66, doi:10.1016/0040-1951(93)90027-H.

Banks, C. J., and J. Warburton (1991), Mid-crustal detachment in the Betic system of the southern Spain, *Tectonophysics*, *191*, 275–289, doi:10.1016/0040-1951(91)90062-W.

Barranco, L. M., J. Ansorge, and E. Banda (1990), Seismic refraction constrains on the geometry of the Ronda peridotite massif (Betic Cordillera, Spain), *Tectonophysics*, *184*, 379–392, doi:10.1016/0040-1951(90)90450-M.

Berástegui, X., C. Banks, C. Puig, C. Taberner, D. Waltham, and M. Fernàndez (1998), Lateral diapiric emplacement of Triassic evaporites at the southern margin of the Guadalquivir Basin, Spain, in *Cenozoic Foreland Basins of Western Europe*, edited by A. Mascle et al., *Geol. Soc. Spec. Publ.*, *134*, 49–68.

Bonini, W. E., T. P. Loomis, and J. D. Robertson (1973), Gravity anomalies, ultramaphic intrusions, and the tectonic of the region around the Straits of Gibraltar, *J. Geophys. Res.*, *78*, 1372–1382, doi:10.1029/JB078i008p01372.

Caldwell, T. G., H. M. Bibby, and C. Brown (2004), The magnetotelluric phase tensor, *Geophys. J. Int.*, *158*(2), 457–469, doi:10.1111/j.1365-246X.2004.02281.x.

Camerlenghi, A., and G. A. Pini (2009), Mud volcanoes, olistostromes and Argille scagliose in the Mediterranean region, *Sedimentology*, *56*(1), 319–365, doi:10.1111/j.1365-3091.2008.01016.x.

Carbonell, R., V. Sallarés, J. Pous, J. J. Dañobeitia, P. Queralt, J. J. Ledo, and V. García-Dueñas (1998), A multidisciplinary geophysical study in the Betic chain (southern Iberia Peninsula), *Tectonophysics*, *288*, 137–152, doi:10.1016/S0040-1951(97)00289-8.

Casas, A., and A. Carbó (1990), Deep structure of the Betic Cordillera derived from the interpretation of a complete Bouguer anomaly map, *J. Geodyn.*, *12*, 137–147, doi:10.1016/0264-3707(90)90003-D.

Chalouan, A., and A. Michard (1990), The Ghomarides nappes, Rif coastal range, Morocco: A Variscan chip in the Alpine belt, *Tectonics*, *9*(6), 1565–1583, doi:10.1029/TC009i006p01565.

Chemenda, A. I., M. Mattauer, and A. N. Bokun (1996), Continental subduction and a mechanism for exhumation of high-pressure metamorphic rocks: New modelling and field data from Oman, *Earth Planet. Sci. Lett.*, *143*, 173–182, doi:10.1016/0012-821X(96)00123-9.

Córdoba, D., E. Banda, and J. Ansorge (1988), P wave velocity-depth distribution in the Hercynian crust of Northwest Spain, *Phys. Earth Planet. Inter.*, *51*, 235–248, doi:10.1016/0031-9201(88)90050-7.

Cowan, D. S. (1985), Structural styles in Mesozoic and Cenozoic mélanges in the western Cordillera of North-America, *Geol. Soc. Am. Bull.*, *96*(4), 451–462, doi:10.1130/0016-7606(1985)96<451:SSIMAC>2.0.CO;2.

Crespo-Blanc, A., and D. Frizon de Lamotte (2006), Structural evolution of the external zones derived from the Flysch trough and the South Iberian and Maghrebian paleomargins around the Gibraltar arc: A comparative study, *Bull. Soc. Geol. Fr.*, *177*(5), 267–282, doi:10.2113/gssgfbull.177.5.267.

Cruz-San Julián, J. (1974), Estudio Geológico del sector Cañete La Real-Teba-Osuna, PhD thesis, 432 pp., Univ. de Granada, Granada, Spain.

Davis, D., J. Suppe, and F. A. Dahlen (1983), Mechanics of fold-and- thrust belts and accretionary wedges, *J. Geophys. Res.*, *88*(B2), 1153–1172, doi:10.1029/JB088iB02p01153.

Durand-Delga, M., P. Rossi, P. Olivier, and D. Puglisi (2000), Structural setting and ophiolitic nature of Jurassic basic rocks associated with the Maghrebian flyschs in the Rif (Morocco) and Sicily (Italy), *C. R. Acad. Sci., Ser. IIa Sci. Terre Planetes*, *331*(1), 29–38.

Egbert, G. D., and J. R. Booker (1986), Robust estimation of geomagnetic transfer functions, *Geophys. J. R. Astron. Soc.*, *87*, 173–194.

Fallot, P. (1948), Les Cordillères Bétiques, *Estud. Geol.*, *4*(7–8), 259–279.

Faure, M., W. Lin, U. Schärer, L. Shu, Y. Sun, and N. Arnaud (2003), Continental subduction and exhumation of UHP rocks. Structural and geochronological insights from the Dabieshan East China, *Lithos*, *70*, 213–241, doi:10.1016/S0024-4937(03)00100-2.

Fernàndez, M., X. Berástegui, C. Puig, D. García Castellanos, M. J. Jurado, M. Torné, and C. Banks (1998), Geophysical and geological constraints on the evolution of the Guadalquivir foreland basin, Spain, in *Cenozoic Foreland Basins of Western Europe*, edited by A. Mascle et al., *Geol. Soc. Spec. Publ.*, *134*, 29–48, doi:10.1144/GSL.SP.1998.134.01.03.

Flinch, J. F., A. W. Bally, and S. Wu (1996), Emplacement of a passive-margin evaporitic allochthon in the Betic Cordillera of Spain, *Geology*, *24*, 67–70, doi:10.1130/0091-7613(1996)024<0067:EOAPME>2.3.CO;2.

Ford, M. (2004), Depositional wedge tops: Interaction between low basal friction external orogenic wedges and flexural foreland basins, *Basin Res.*, *16*, 361–375, doi:10.1111/j.1365-2117.2004.00236.x.

Galindo-Zaldívar, J., A. Jabaloy, F. González-Lodeiro, and F. Aldaya (1997), Crustal structure of the central sector of the Betic Cordillera (SE Spain), *Tectonics*, *16*, 18–37, doi:10.1029/96TC02359.

Galindo-Zaldívar, J., F. González-Lodeiro, A. Jabaloy, A. Maldonado, and A. A. Schreider (1998), Models of magnetic and Bouguer gravity anomalies for the deep structure of the central Alboran Sea basin, *Geo Mar. Lett.*, *18*, 10–18, doi:10.1007/s003670050046.

García-Castellanos, D., M. Fernàndez, and M. Torné (2002), Modeling the evolution of the Guadalquivir foreland basin (southern Spain), *Tectonics*, *21*(3), 1018, doi:10.1029/2001TC001339.

García-Dueñas, V. (1969), Les unités allochtones de la Zone Subbétique, dans la transversale de Grenade (Cordillères Bétiques, Espagne), *Rev. Geogr. Phys. Geol. Dyn.*, *11*(2), 211–222.

García-Hernández, M., A. C. López-Garrido, P. Rivas, C. Sanz de Galdeano, and J. A. Vera (1980), Mesozoic palaeogeographic evolution of the external zones of the Betic Cordillera, *Geol. Mijnbouw*, *59*(2), 155–168.

Hsü, K. J. (1968), Principles of mélanges and their bearing on the Franciscan-Knoxville paradox, *Geol. Soc. Am. Bull.*, *79*, 1063–1074, doi:10.1130/0016-7606(1968)79[1063:POMATB]2.0.CO;2.

Instituto Geográfico Nacional (IGN) (1976), *Mapa de Anomalías de Bouguer. Escala 1:1.000.000*, Madrid.

Instituto Geológico y Minero de España (IGME) (1987), *Contribución de la Exploración Petrolífera al Conocimiento de la Geología de España*, 465 pp., Madrid.

Jaumé, S. C., and R. J. Lillie (1988), Mechanics of the Salt Ranges-Potwar Plateau, Pakistan: A fold-and-thrust belt underlain by evaporites, *Tectonics*, *7*, 57–71, doi:10.1029/TC007i001p00057.

Lickorish, W. H., M. Grasso, R. W. H. Butler, A. Argnani, and R. Maniscalco (1999), Structural styles and regional tectonic setting of the "Gela Nappe" and frontal part of the Maghrebian thrust belt in Sicily, *Tectonics*, *18*(4), 655–668, doi:10.1029/1999TC900013.

Lonergan, L. (1993), Timing and Kinematics of deformation in the Malaguide Complex, Internal Zone of the Betic Cordillera, Southeast Spain, *Tectonics*, *12*(2), 460–476, doi:10.1029/92TC02507.

Lonergan, L., and N. White (1997), Origin of the Betic-Rif mountain belt, *Tectonics*, *16*(3), 504–522, doi:10.1029/96TC03937.

Luján, M., F. Storti, J. C. Balanyá, A. Crespo-Blanc, and F. Rossetti (2003), Role of décollement material with different rheological properties in the structure of the Aljibe thrust imbricate (Flysch Trough, Gibraltar Arc): An analogue modelling approach, *J. Struct. Geol.*, *25*(6), 867–881, doi:10.1016/S0191-8141(02)00087-1.

Mariotti, G., and C. Doglioni (2000), The dip of the foreland monocline in the Alps and Apennines, *Earth Planet. Sci. Lett.*, *181*, 191–202, doi:10.1016/S0012-821X(00)00192-8.

Martí, A., P. Queralt, and E. Roca (2004), Geoelectric dimensionality in complex geological areas: Application to the Spanish Betic Chain, *Geophys. J. Int.*, *157*(3), 961–974, doi:10.1111/j.1365-246X.2004.02273.x.

Martí, A., P. Queralt, E. Roca, J. Ledo, and J. Galindo-Zaldivar (2009), Geodynamic implications for the formation of the Betic-Rif orogen from magnetotelluric studies, *J. Geophys. Res.*, *114*, B01103, doi:10.1029/2007JB005564.

Matte, P., M. Mattauer, J. M. Olivet, and D. A. Griot (1997), Continental subductions beneath Tibet and the Himalayan orogeny: A review, *Terra Nova*, *9*, 264–270, doi:10.1111/j.1365-3121.1997.tb00026.x.

Mazzoli, S., and A. M. Algarra (2011), Deformation partitioning during transpressional emplacement of a 'mantle extrusion wedge': The Ronda peridotites, western Betic Cordillera, Spain, *J. Geol. Soc.*, *168*(2), 373–382, doi:10.1144/0016-76492010-126.

Medialdea, T., E. Suriñach, R. Vegas, E. Banda, and J. Ansorge (1986), Crustal structure under the western end of the Betic cordillera (Spain), *Ann. Geophys.*, *4*(4), 457–464.

Monteiro Santos, F. A., J. Pous, E. P. Almeida, P. Queralt, A. Marcuello, H. Matias, and L. A. M. Victor (1999), Magnetotelluric survey of the electrical conductivity of the crust across the Ossa Morena Zone and South Portuguese Zone suture, *Tectonophysics*, *313*(4), 449–462, doi:10.1016/S0040-1951(99)00209-7.

Monteiro Santos, F. A., A. Mateus, E. P. Almeida, J. Pous, and L. A. Mendes-Victor (2002), Are some of the deep crustal conductive features found in SW Iberia caused by graphite?, *Earth Planet. Sci. Lett.*, *201*(2), 353–367, doi:10.1016/S0012-821X(02)00721-5.

Moore, G. F., and D. E. Karig (1980), Structural geology of Nias Island, Indonesia: Implications for subduction zone tectonics, *Am. J. Sci.*, *280*, 193–223, doi:10.2475/ajs.280.3.193.

Morales, J., I. Serrano, A. Jabaloy, J. Galindo-Zaldívar, D. Zhao, F. Torcal, F. Vidal, and F. González-Lodeiro (1999), Active continental subduction beneath the Betic Cordillera and the Alboran Sea, *Geology*, *27*(8), 735–738, doi:10.1130/0091-7613(1999)027<0735:ACSBTB>2.3.CO;2.

Munhá, J., J. T. Oliveira, A. Ribeiro, V. Oliveira, C. Quesada, and R. Kerrich (1986), Beja-Acebuches ophiolite, characterization and geodynamic significance, *Maleo*, *2*, 31.

Oliveira, J. T. (1990), Stratigraphy and syn-sedimentary tectonism in the South Portuguese Zone, in *Pre-Mesozoic Geology of Iberia*, edited by D. Dallmeyer and E. Martinez, pp. 334–347, Springer, Berlin, doi:10.1007/978-3-642-83980-1_23.

Parkinson, W. D. (1962), The influence of continents and oceans on geomagnetic variations, *Geophys. J. R. Astron. Soc.*, *6*(4), 441–449, doi:10.1111/j.1365-246X.1962.tb02992.x.

Pedley, R. C., J. P. Busby, and Z. K. Dabeck (1993), GRAVMAG User Manual-Interactive 2.5D gravity and magnetic modeling, *Tech. Rep. WK/93/26/R*, Br. Geol. Surv., Nottingham, U. K.

Pedrera, A., J. Galindo-Zaldívar, A. Ruiz-Constán, C. Duque, C. Marin-Lechado, and I. Serrano (2009), Recent large fold nucleation in the upper crust: Insight from gravity, magnetic, magnetotelluric and seismicity data (Sierra de Los Filabres-Sierra de Las Estancias, Internal Zones, Betic Cordillera), *Tectonophysics*, *463*(1–4), 145–160, doi:10.1016/j.tecto.2008.09.037.

Pedrera, A., et al. (2010), Crustal-scale transcurrent fault development in a weak-layered crust from an integrated geophysical research: The Carboneras Fault Zone (eastern Betic Cordillera, Spain), *Geochem. Geophys. Geosyst.*, *11*, Q12005, doi:10.1029/2010GC003274.

Pedrera, A., C. Marín-Lechado, S. Martos-Rosillo, and F. J. Roldán (2012), Curved fold-and-thrust accretion during the extrusion of a synorogenic viscous allochthonous sheet: The Estepa Range (External Zones, Western Betic Cordillera, Spain), *Tectonics*, doi:10.1029/2012TC003119, in press.

Perconig, E. (1960–1962), Sur la constitution géologique de l'Andalousie occidentale, en particulier du bassin du Guadalquivir (Espagne méridionale), in *Livre à la Mémoire du Professeur Paul Fallot*, *Mem. Hors Ser. Soc. Geol. Fr.*, *1*, 231–256.

Pérez López, A., and C. Sanz de Galdeano (1994), Tectónica de los materiales triásicos en el sector central de la Zona Subbética (Cordillera Bética), *Rev. Soc. Geol. Esp.*, *7*(1–2), 141–153.

Pini, G. A. (1999), Tectonosomes and olistostromes in the Argille Scagliose of the Northern Apennines, Italy, *Spec. Pap. Geol. Soc. Am.*, *335*, 1–70.

Platt, J. P., S. Allerton, A. Kirker, C. Mandeville, A. Mayfield, E. S. Platzman, and A. Rimi (2003), The ultimate arc: Differential displacement, oroclinal bending, and vertical axis rotation in the External Betic-Rif arc, *Tectonics*, *22*(3), 1017, doi:10.1029/2001TC001321.

Polyak, B. G., et al. (1996), Heat flow in the Alboran Sea, western Mediterranean, *Tectonophysics*, *263*, 191–218.

Pous, J., P. Queralt, J. Ledo, and E. Roca (1999), A high electrical conductive zone at lower crustal depth beneath the Betic Chain (Spain), *Earth Planet. Sci. Lett.*, *167*, 35–45, doi:10.1016/S0012-821X(99)00011-4.

Pous, J., G. Muñoz, W. Heise, J. C. Melgarejo, and C. Quesada (2004), Electromagnetic imaging of Variscan crustal structures in SW Iberia: The role of interconnected graphite, *Earth Planet. Sci. Lett.*, *217*(3–4), 435–450, doi:10.1016/S0012-821X(03)00612-5.

Raymond, L. A. (1984), Classification of mélanges, in *Mélanges: Their Nature, Origin, and Significance*, edited by L. A. Raymond, *Spec. Pap.Geol. Soc. Am.*, *198*, 7–20.

Rodi, W., and R. L. Mackie (2001), Nonlinear conjugate gradients algorithm for 2-D magnetotelluric inversion, *Geophysics*, *66*(1), 174–187, doi:10.1190/1.1444893.

Roldán, F. J., J. Rodríguez-Fernández, and J. M. Azañón (2012), The Olistostromic Unit, a key formation to understand the Neogene history of the Betic Cordillera External Zones, *Geogaceta*, in press.

Roldán García, F. J. (1995), Evolución neógena de la Cuenca del Guadalquivir, PhD thesis, 259 pp., Univ. of Granada, Granada, Spain.

Rosell, O., A. Martí, A. Marcuello, J. Ledo, P. Queralt, E. Roca, and J. Campanya (2011), Deep electrical resistivity structure of the northern Gibraltar Arc (western Mediterranean): Evidence of lithospheric slab break-off, *Terra Nova*, *23*(3), 179–186, doi:10.1111/j.1365-3121.2011.00996.x.

Ruiz-Constán, A., J. Galindo-Zaldívar, A. Pedrera, and C. Sanz de Galdeano (2009), Gravity anomalies and orthogonal box fold development on heterogeneous basement in the Neogene Ronda Depression (Western Betic Cordillera), *J. Geodyn.*, *47*(4), 210–217, doi:10.1016/j.jog.2008.09.004.

Ruiz-Constán, A., J. Galindo-Zaldívar, A. Pedrera, J. A. Arzate, J. Pous, F. Anahnah, W. Heise, F. A. M. Santos, and C. Marin-Lechado (2010), Deep deformation pattern from electrical anisotropy in an arched orogen (Betic Cordillera, western Mediterranean), *Geology*, *38*(8), 731–734, doi:10.1130/G31144.1.

Ruiz-Constán, A., J. Galindo-Zaldívar, A. Pedrera, B. Célérier, and C. Marin-Lechado (2011), Stress distribution at the transition from subduction to continental collision (northwestern and central Betic Cordillera), *Geochem. Geophys. Geosyst.*, *12*, Q12002, doi:10.1029/2011GC003824.

Sánchez Jiménez, N. (2004), Estructura gravimétrica y magnética de la corteza del suroeste peninsular (zona surportuguesa y zona de Ossa-Morena), PhD thesis, 243 pp., Univ. Complutense de Madrid, Madrid.

Sanz de Galdeano, C. (1975), *Geología de la Transversal Jaén-Frailes (Provincia de Jaén)*, 274 pp., Univ. de Granada, Granada, Spain.

Sanz de Galdeano, C., and J. A. Vera (1992), Stratigraphic record and palaeogeographical context of the Neogene basins in the Betic Cordillera, Spain, *Basin Res.*, *4*, 21–36, doi:10.1111/j.1365-2117.1992.tb00040.x.

Serrano, F. (1979), Los foraminíferos planctónicos del Mioceno superior de la cuenca de Ronda y su comparación con los de otras áreas de la Cordilleras Béticas, PhD thesis, 272 pp., Univ. de Málaga, Málaga, Spain.

Simancas, J. F., D. M. Poyatos, I. Exposito, A. Azor, and F. González-Lodeiro (2001), The structure of a major suture zone in the SW Iberian Massif: The Ossa-Morena/Central Iberian contact, *Tectonophysics*, *332*(1–2), 295–308, doi:10.1016/S0040-1951(00)00262-6.

Staub, R. (1934), Der Deckenbau Südspaniens in den Betischen Cordilleren, *Viert. Nat. Ges. Zurich*, *79*, 271–332.

Suriñach, E., and R. Vegas (1988), Lateral inhomogeneities of the Hercyninan crust in central Spain, *Phys. Earth Planet. Inter.*, *51*, 226–234, doi:10.1016/0031-9201(88)90049-0.

Talbot, C. J., and M. Alavi (1996), The past and future syntaxis across the Zagros, in *Salt Tectonics*, edited by G. I. Alsop, D. J. Blundell, and I. Davison, *Geol. Soc. Spec. Publ.*, *100*, 89–109, doi:10.1144/GSL.SP.1996.100.01.08.

Telford, W. M., L. P. Geldart, and R. E. Sheriff (1990), *Applied Geophysics*, 770 pp., Cambridge Univ. Press, Cambridge, U. K., doi:10.1017/CBO9781139167932.

Torné, M., and E. Banda (1992), Crustal thinning from the Betic Cordillera to the Alboran Sea, *Geo Mar. Lett.*, *12*(2–3), 76–81, doi:10.1007/BF02084915.

Torné, M., E. Banda, V. García-Dueñas, and J. C. Balanyá (1992), Mantle-lithosphere bodies in the Alboran crustal domain (Ronda Peridotites, Betic Rif Orogenic Belt), *Earth Planet. Sci. Lett.*, *110*(1–4), 163–171, doi:10.1016/0012-821X(92)90046-X.

Tubía, J. M., J. Cuevas, F. Navarro-Vilá, F. Alvarez, and F. Aldaya (1992), Tectonic evolution of the Alpujarride Complex (Betic Cordillera, Southern Spain), *J. Struct. Geol.*, *14*(2), 193–203, doi:10.1016/0191-8141(92)90056-3.

Vannucchi, P., and G. Bettelli (2002), Mechanisms of subduction accretion as implied from the broken formations in the Apennines, Italy, *Geology*, *30*(9), 835–838, doi:10.1130/0091-7613(2002)030<0835:MOSAAI>2.0.CO;2.

Vera, J. A. (2004), Zonas Externas Béticas, in *Geología de España*, edited by J. A. Vera, pp. 354–389, Soc. Geol. de Esp.-Inst. Geol. y Min. de Esp., Madrid.

Vozoff, K. (1972), The magnetotelluric method in the exploration of sedimentary basins, *Geophysics*, *37*(1), 98–141.

Working Group for Deep Seismic Sounding in Alboran 1974 (1978), Crustal seismic profiles in the Alboran Sea preliminary results, *Pure Appl. Geophys.*, *116*, 167–180, doi:10.1007/BF00878991.